Antibody-mediated inhibition of syndecan-4 dimerization reduces interleukin (IL)-1 receptor trafficking and signaling.

Lars Godmann[1], Miriam Bollmann[2], Adelheid Korb-Pap[1], Ulrich König[1], Joanna Sherwood[1], Denise Beckmann[1], Katja Mühlenberg[1], Frank Echtermeyer[1, 3], James Whiteford[4], Giulia De Rossi[4], Thomas Pap[1#], Jessica Bertrand[2]

[1]Institute of Musculoskeletal Medicine (IMM), University Muenster, Muenster, Germany; [2]Department of Orthopaedic Surgery, Otto-von-Guericke University Magdeburg, Germany; [3]Department of Anesthesiology and Intensive Care Medicine, Hannover Medical School, Germany;

[4]Centre for Microvascular Research, Queen Mary University of London, UK

Word count: 3.983

[#]Corresponding author:
Thomas Pap, MD,
Institute of Musculoskeletal Medicine (IMM),
University Hospital Muenster,
Albert Schweitzer-Campus 1, Building D3,
D-48149 Muenster, Germany,
Email: thomas.pap@uni-muenster.de
Tel: +49 (251) 83 57798

Abstract

Objective: Syndecan-4 (sdc4) is a cell-anchored proteoglycan that consists of a transmembrane core protein and glucosaminoglycan (GAG) side chains. Binding of soluble factors to the GAG-chains of sdc4 may result in the dimerization of sdc4 and the initiation of downstream signaling cascades. However, the question of how sdc4 dimerization and signaling affects the response of cells to inflammatory stimuli is unknown.

Methods: Sdc4 immunostaining was performed on rheumatoid arthritis (RA) tissue sections. Interleukin (IL)-1 induced ERK phosphorylation and MMP3 production was investigated. Il-1 binding to sdc4 was investigated using immunoprecipitation. IL-1 receptor (IL-1R) staining on wildtype, sdc4 and il1R1 knockout fibroblasts was performed in FACS analyses. A blocking sdc-4 antibody was used to investigate sdc-4 dimerization, il1-R1 expression and the histological paw destruction in the hTNFtg mouse.

Results: We show that in fibroblasts the loss of sdc4 or the antibody-mediated inhibition of sdc4 dimerization reduces the cell surface expression of the IL-1R and regulates the sensitivity of fibroblasts to IL-1. We demonstrate that IL-1 directly binds to sdc4 and in an IL-1R independent manner leads to its dimerization. IL-1 induced dimerization of Sdc4 regulates caveolin vesicle-mediated trafficking of the IL-1R1, which in turn determines the responsiveness to IL-1. Administration of antibodies against the dimerization domain of sdc4, thus, strongly reduces the expression IL-1R1 on arthritic fibroblasts both *in vitro* and an animal model of human rheumatoid arthritis.

Conclusion: Collectively, our data suggest that antibodies that specifically inhibit sdc4 dimerization may support anti-IL-1 strategies in diseases such as inflammatory arthritis.

Introduction:

Human rheumatoid arthritis (RA) is a systemic autoimmune disease that primarily affects the joints and that is characterized by chronic inflammation, progressive cartilage destruction and bone erosions [1]. Resident fibroblast-like synoviocytes (FLS) in the joints have been implicated prominently in the progression of disease, in which early cartilage damage appears to be of pivotal importance [2]. These FLS exhibit an autonomously aggressive phenotype that is maintained in the absence of continuous inflammatory stimulation [3]. The transformation of FLS in rheumatoid arthritis is associated with altered secretion of soluble factors such as cytokines and chemokines as well as an enhanced response to inflammatory mediators such as IL-1. Although clinical studies targeting IL-1 have shown only limited efficacy in established disease [4], a number of studies using both pharmacological inhibition of IL-1 and IL-1-deficient mice have identified IL-1 as an important trigger of early arthritic cartilage damage with FLS being both an important source of and target cell for IL-1 [5]. We have shown previously that the loss of syndecan-4 (sdc4) protects mice from cartilage damage in animal models of osteoarthritis [6] and RA [7]. In this context, we also showed that chondrocytes lacking sdc4 exhibited a reduced responsiveness to IL-1 with reduced IL-1 mediated ERK phosphorylation [6]. In these studies, antibodies raised against the dimerization domain of sdc4 exhibited a blocking effect on IL-1 induced ERK signalling but the mechanism by which the loss or inhibition of sdc4 interfered with IL1 signaling remains unclear [6]. Interestingly, recent evidence suggests that trafficking of the IL1-receptor (IL-1R1) involves the formation of caveolin vesicles [8] and that sdc4 may regulate the caveolin-mediated endocytosis of signaling molecules such as Rac1 [9] as well as of cell surface receptors such as integrins [10].

Based on these data we studied the mechanisms by which sdc4 regulates IL-1 signaling and explored the possibility of specifically interfering with sdc4 regulated IL-1 signaling through the delivery of specific antibodies. We report that IL-1 binds to sdc4 and leads to its dimerization which regulates caveolin vesicle-mediated trafficking of IL-1R1. Administration of antibodies against the dimerization domain of sdc4, thus, strongly desensitizes arthritic fibroblasts against IL-1, providing a novel tool for therapeutic intervention in IL-1 mediated diseases.

Results

Scd4 reduces IL-1ß signalling by direct binding to the heparan sulphate (HS) side chains and induction of sdc4 dimerization

We first investigated the expression of sdc4 in human RA as well as in the human TNFalpha transgenic (hTNFtg) mouse, an established animal model of the disease. As shown in Fig. 1a, scd4 was highly expressed in RA synovium, with very prominent staining in the most

superficial lining layer that mediates the attachment to and degradation of articular cartilage. In contrast, only very few scd4 expressing cells were found in synovial tissues from OA patients. As determined by quantitative real-time PCR, the upregulation was also evident at the mRNA level, where RASF expressed 3.5-fold higher levels of scd4 than OASF. These data suggested that the inflammatory environment in the RA synovium leads to a strong and sustained upregulation of scd4 in synovial fibroblasts. To further investigate if chronic exposure to TNFalpha results in a sustained upregulation of scd4 in synovial fibroblasts, hTNFtg mice were analyzed for the expression of scd4. As seen in immunohistochemistry, there was a strong expression of scd4 in the synovial membranes of hTNFtg (Fig. 1b) mice, whereas only negligible staining for scd4 was found in synovial tissues of wild type animals. *In vitro*, synovial fibroblasts isolated from hTNFtg mice showed more than 21.6-fold higher expression of scd4 than wild type controls (Fig. 1b).

TNFα and IL-1β both have been shown to be of importance for FLS activation in RA. In Western blot analyses, we found that loss of Sdc4 in FLS did not affect of ERK activation in response to TNF alpha (Fig. 1c). However, Sdc4 deficiency in FLS significantly reduced IL-1ß dependent phosphorylation of ERK1/2 (Figure 1d). Next, we asked the question if reduction in IL-1β induced ERK- signalling in Sdc4-/- FLS would translate into reduced expression of disease-relevant matrix metalloproteinases (MMPs). When investigating the expression of MMP-3 in cell culture supernatants of TNFα and IL-1ß stimulated FLS from wild type and Sdc4-/- mice we found that, again, TNF alpha induced expression of MMP-3 was not different between wild type and Sdc4-/- FLS (Fig. 1e). However, stimulation of Sdc4-/- FLS with IL-1ß led to significantly lower levels of MMP-3 compared to those from IL-1 stimulated wild type controls (wt: 151.41 ± 5.02, Scd4-/-: 77.13 ± 8.36, p=0.001)(Fig. 1f).

These findings made us wonder whether there is a direct interaction between Sdc4 and the cytokines IL-1ß and TNFα. To this end, we transfected HEK cells either with FLAG tagged full length sdc4 (flag-sdc4wt) or with a FLAG-tagged mutant of sdc4 lacking the attachment sites for GAG side chains (flag-sdc4S3A). We found that unlike TNF alpha, which showed no interaction with either flag-sdc4wt or with flag-sdc4S3A, IL-1β bound to flag-sdc4wt but not to flag-sdc4S3A (Fig. 1g), indicating that the GAG chains of Sdc4 mediated the binding of IL-1. Next, we were interested to see if IL-1β could induce dimerization of Sdc4, which has been described to be a key step in sdc4 mediated signal transduction [11]. Interestingly, IL-1β induced dimerization of sdc4 was also observed in FLS lacking the IL-1R1 (Fig. 1h), suggesting that the dimerization of sdc4 is a direct effect of IL-1 binding and not a secondary effect due to IL-1 receptor signalling. As shown in Fig. 1i, stimulation of NIH3T3 fibroblasts with IL-1 resulted in dimerization of sdc4, which was stabilized using the chemical cross-linker BS^3. Obviously no dimers were detectable in the $Sdc4^{-/-}$ fibroblasts and in unstimulated

NIH/3T3 fibroblasts even after crosslinking. Wildtype FLS transfected with wt-sdc4-plasmid served as positive control.

Sdc4 regulates IL1R1 trafficking upon Il-1 stimulation

These data made us wonder about the mechanisms by which sdc4 regulates the sensitivity of FLS to IL-1. Using flow cytometry analyses, we found that the loss of sdc4 was associated with a significant reduction of IL1R1 surface expression on FLS (wt: 9.77 ± 0.77, sdc4: 1.94 ± 0.19, IL-1R1: 0.52 ± 0.04, p=0.0006) (Fig. 2a). Importantly, mRNA levels of IL-1R1 were unaltered in sdc4$^{-/-}$ cells compared to wt (Fig. 2b), indicating that sdc4 does not regulate IL1R1 expression but rather affects translational processes and/or trafficking of the IL1R1. The lack of sdc4 had no influence on the expression of the TNF receptor 1 (TNFR1) either on the cell surface as determined by FACS analysis (wt: 7.38 ± 0.5, sdc4: 7.47 ± 0.43, IL-1R1: 8.47 ± 0.20, p= 0.9056) (Fig. 2c), or at the mRNA level (Fig. 1d). To investigate the time kinetics of IL1R1 surface presentation we performed FACS analyses of the IL1R1 at 10 minutes as well as, 3 and 5 hours following IL-1 stimulation. We observed a significant reduction in Il1R1 at the cell surface in wt fibroblasts after 10 minutes (0.92 ± 0.02, p= 0.0286), which was recovered after 3 hours (1.04 ± 0.07). This effect was not observed in sdc4-/- fibroblasts (sdc4 t10: 0.89 ± 0.04, sdc4 t3h: 0.85 ± 0.04) (Fig. 2e). Because the trafficking of the IL1R1 involves the formation of caveolin vesicles, we next investigated whether inhibition of caveolin vesicle formation either by treatment with Nystatin or by siRNA has similar effects on IL-1 induced ERK phosphorylation as the knockout or inhibition of sdc4. Indeed, when we treated wild type FLS with Nystatin, FLS lost their ability to respond to IL-1 with a phosphorylation of ERK (Fig. 2f). As Caveolin-1 (Cav-1) is a key component of caveolin vesicles (16), and phosphorylation of Cav-1 constitutes a key step in caveolin vesicle translocation (17), we also knocked down Cav-1 with specific siRNA and found that Cav-1 deficient FLS, in a similar way as Nystatin treated cells, lost their ability to phosphorylate ERK in response to IL-1 (Fig. 2g). In line with these observations, treatment of wt FLS with Nystatin, significantly reduced the presentation of the IL1R1 on the cell surface (wt: 6.15 ± 0.40, wt nystatin: 3.31 ± 0.11, p=0.009), but had only minor additional effects on sdc4 deficient cells (Sdc4: 3.90 ± 0.27, Sdc4 nystatin: 2.58 ± 0.19) (Fig. 2h). At the mRNA level, we found no differences in Cav-1 expression between wt and sdc4-/- FLS (wt: 0.99 ± 0.17, sdc4: 0.99 ± 0.18, p= 0.995) (Fig. 2i). However, when studying the presence of phosphorylated Cav-1 by sucrose gradient centrifugation, we found that sdc4-/- FLS contain far less phospho-Cav-1 than wt cells after stimulation with IL-1 beta (Fig. 2j).

Sdc4 blocking antibody reduces IL1R1 surface presentation leading to reduced RA symptoms in the hTNFtg RA mouse model

As these data indicated that sdc4 is an important regulator of IL-1 signaling, we tested whether the application of specific antibodies (Ab) raised against the extracellular dimerization motif of sdc4 [6, 12] would result in a reduction of ERK phosphorylation as a marker for IL-1 signalling activation. Incubation of FLS with the blocking Ab clearly inhibited the IL-1 induced ERK-1/2 phosphorylation to a comparable extent as the loss of Sdc4 (Fig. 3a). Moreover FACS analyses of FLS treated with the blocking Sdc4 Ab or IgG revealed that anti-sdc4-Ab treated cells exhibited less IL1R1 on their surface than did IgG treated FLS (wt: 7.30 ± 0.29, sdc4: 4.29 ± 0.21, p=0.001) (Fig. 3b).

Additionally, we observed a reduction in Sdc4 dimers as early as 5 minutes after IL-1 stimulation (untreated: 1.27 ± 0.30, IL-1: 0.36 ± 0.13, p= 0.0091) (Fig. 3c). These data indicate that the dimerization of sdc4 is involved in IL1R1 trafficking after IL-1 stimulation. Incubation of FLS with the blocking scd4 Ab or the combination of IL-1 and the blocking scd4 Ab exhibited no additional effect (Fig. 3c).

These data raised the question of whether the timely application of our blocking anti-sdc4 antibodies downregulates IL-1R1 and prevents cartilage destruction in human TNFα transgenic (hTNFtg) mice to a similar extent as we found in Scd4-/- mice previously [7] and as also observed in mice that lack IL-1R1. Indeed, injection of the antibodies into eight week old hTNFtg mice three times per week for four weeks protected the treated joints nearly completely from cartilage damage (Fig. 3d) with decreased pannus area (IgG:21.92 ± 3.63, α-Sdc4-Ab:6.795 ± 2.56, p= 0.0144, n=4), cartilage erosion (IgG: 36.19 ± 4.96, α-Sdc4-Ab:10.19 ± 3.99, p= 0.0065, n=4), decreased proteoglycan loss (IgG: 68.82 ± 4.17, α-Sdc4-Ab: 18.14 ± 4.47, p= 0.0002, n=4) and decreased expression of MMP-3 (IgG: 4.43 ± 0.62, α-Sdc4-Ab: 0.68 ± 0.48, p= 0.0007, n=4) (Fig. 3d). The extent to which the antibody inhibited cartilage damage was comparable to that in hTNFtg mice that lacked Sdc4 (10) or IL-1R1 (Fig. 3d). This was also seen in histomorphometric analyses, where the inhibition of sdc4 and the loss of the IL-1R1 gave very similar results those from the hTNFtg background (Fig. 3d).

Discussion

In this work, we have investigated how sdc4 modulates the response of fibroblasts to the inflammatory cytokine IL-1 and asked the question if specific, antibody-mediated targeting of sdc4 may alter the response of fibroblasts to IL-1, particularly during chronic destructive arthritis. Since various proteins have been found to bind to the GAG chains of sdc4 [13], and IL-1ß binding to GAG chains of both the heparan sulfate type and the chondroitin sulfate type have been described before [14], the demonstration that IL-1 can bind to the side chains of Sdc4 was no surprise. However, we could show that binding of IL-1 to the sdc4 GAG chains also results in the dimerization of sdc4 which has been suggested to constitute a prerequisite for sdc4- mediated intracellular signaling [15, 16]. This is of importance because a clear

function of the extracellular domain in dimerization had not previously been shown, while in our studies Abs against the dimerization domain of sdc4 not only inhibited dimer formation but also reduced IL-1 induced ERK phosphorylation in a similar way as did the loss of sdc4, suggesting that sdc4 dimer formation by itself facilitates the IL-1 response of fibroblasts. It may be hypothesised that IL-1 induced dimerization of sdc4 results from the interaction of IL-1 with its cognate receptor rather than from the direct binding of IL-1 to sdc4. This was not seen when whole cell lysates were used, most likely reflecting the dynamics of sdc4 internalisation in response to IL-1. However, dimerization of sdc4 in response to IL-1 was also seen in IL-1R deficient cells, suggesting that the IL-1R is not required for IL-1 to induce scd4 dimerization and, thus, signaling through this pathway. Recent data suggest that trafficking of the IL-1R1 involves the formation of caveolin vesicles [8]. In line with these data, we found that the inhibition of caveolin vesicle formation either by treatment with Nystatin [17] or through RNAi has similar effects on IL-1 induced ERK phosphorylation as had the knockout of sdc4 or the Ab- mediated inhibition of sdc4 dimerization. An interaction of Sdc4 with caveolin vesicles has been previously proposed [18], and it has been shown that sdc4 is involved prominently in caveolin-mediated integrin recycling. In line with these findings, we detected a reduced presence of IL1R1 on the cell surface in sdc4 deficient fibroblasts, which was dependent on caveolin vesicle formation. The time course of IL1R1 surface presentation in combination with Sdc4 dimer detection indicate that the presence of Sdc4 critically regulates the surface presentation of IL1R1. Thus it may be hypothesised that upon induction of IL1 signaling, the IL1R1 is reduced from the cell surface at the same time as Sdc4 dimerization is reduced. To show the *in vivo* relevance of the described mechanism, we applied the blocking anti-sdc4 antibody to hTNFtg mice that are a model for human RA disease. Importantly, treatment with the blocking antibody resulted in a similar phenotype as found in the IL1R1 knockout, as well as the Sdc4-/- hTNFtg mouse [7]. However, the effect of the blocking sdc4-antibody was not as strong, as the effect of the complete knockout, which might be explained by residual sdc4 on the cell surface that was not blocked by the sdc4 antibody, as we did not titrate for the maximum effect of the blocking antibody.

Collectively, our data demonstrate that dimerization of sdc4 is critically involved in IL1 signal transduction and IL1R1 surface presentation via caveolin-dependent mechanisms and those antibodies that specifically inhibit sdc4 dimerization may support anti-IL-1 strategies in diseases such as inflammatory arthritis.

Materials and Methods

Blocking sdc4 antibodies

The blocking sdc4 antibodies were generated against the peptide NAQPGIRVPSEPKELEENEVIPKRAPSDV of the extracellular part of sdc-4. Rabbits were immunized with the synthetic peptide and the antibodies were purified by Pineda (Berlin, Germany). The polyclonal antibodies of two different immunized rabbits were tested for sdc4 specificity using western blot (suppl. Fig 1 and c). The specificity of the antibody used for the treatment of hTNFtg mice was also tested in immunohistological stainings of wt and sdc4 ko fibroblasts (suppl. fig 1 b). To test the reproducibility of generating blocking sdc4 antibodies when using the extracellular part of sdc4 for immunization, we tested the polyclonal antibodies of another immunized rabbit for the capability to inhibit IL-1 induced ERK1/2 phosphorylation (representative western blot, suppl. fig 1d).

Animals and treatment

hTNFtg mice (strain Tg197) have been described previously [19] and were maintained on the C57BL/6 genetic background. We generated all data from sex and age-matched littermates. The hind paws of eight week old hTNFtg mice were either treated with our blocking sdc4 antibodies or an IgG control (Chrome Pure Rabbit IgG, Dianova) by p.a. injections of 50 µl into the hind paw, three times weekly for four weeks. Afterwards, mice were euthanised and the hind paws were prepared for histological analysis. All animal experiments were authorised by the Animal Use Committee in Muenster under the file reference 84-02.04.2014.A465.

Arthritis assessment

Histological analysis was conducted on 4% phosphate-buffered paraformaldehyde-fixed, decalcified paraffin sections of hind paw joints. Paraffin sections were stained with toluidine blue. Quantification of pannus area, destained cartilage and cartilage erosion were performed using a Zeiss Observer Z1 microscope (Carl Zeiss) and the Zeiss AxioVision 4.7.1 software.

Immunohistochemistry

MMP-3 staining was performed using anti-MMP-3 antibody (Abcam) and subsequent detection using the alkaline phosphatase reagent from the Vector Red SK-5100 substrate (Vector Laboratories). For IL-1R staining, the anti-IL-1R antibody (Bioss) was used. The staining was visualized using the DAB reagent from the DAB Peroxidase (HRP) kit SK-4100 (Vector Laboratories). Quantification was performed using Image-Pro Plus. IL-1R positive cells (%) were measured by dividing the number of positive stained cells by the total cell number. To calculate the MMP-3 positive joint area (%) a rectangle of fixed size was laid over each joint and the positive stained area was divided by the total area of the rectangle.

Histology

All studies were approved by the ethics committees of the University Hospital Muenster. Samples of synovial tissues from patients with RA or OA were obtained from joint replacement surgery (Ethics committee Muenster, approval number 2009-049-f-s). Tissue samples from RA and OA patients were fixed in 4% paraformaldehyde overnight, embedded into paraffin and sectioned into 5 µm slices. Tissue sections were pre-treated with 1x Trypsin/EDTA (PAA Laboratories, Pasching, Austria) for 20min at 37°C, blocked with 10% horse serum and stained with a monoclonal scd4 antibody (Santa Cruz, clone 5G9) for human tissue sections over night at 4°C. Immunohistochemistry was performed with an alkaline phosphatase technique using Vectastain ABC-A, Vector Red Substance and secondary biotinylated antibodies (Vector Laboratories, Burlingame, CA). Nuclei were counterstained with methyl green (Vector Laboratories, Burlingame, CA).

Immunocytochemistry

RASF and OASF were seeded on glass cover slips, fixed with 4% paraformaldehyde including 0.1% Tween 20, blocked with 1% BSA and stained with the monoclonal scd4 antibody 5G9 and an Alexa488 goat anti-mouse antibody (Molecular Probes) for detection of scd4 expression. Propidium iodide (Sigma) was used to stain the nuclei.

Murine synovial fibroblasts

Murine synovial fibroblasts were isolated from hind paws. Joints were dissociated and digested with Collagenase IV (Worthington) and cultured in DMEM (Sigma) supplemented with 10 % FCS (PAA). The murine fibroblast cell line NIH/3T3 was used for transfection experiments. All cells were cultured in DMEM with 10% FCS at 37°C and 5% CO2 until passages 4-6. Cells were stimulated for the indicated time period with 10 ng/ml murine IL-1 beta (R&D systems) or 10 ng/ml human TNF alpha (R&D systems).

Immunoprecipitation

Immunoprecipitation was performed using Anti-FLAG M2 Magnetic Beads (Sigma) according to the manufacturer's protocol. Therefore, we transfected HEK cells either with FLAG tagged full length sdc4 (flag-sdc4wt) or with a FLAG-tagged mutant of sdc4 in which all GAG binding serine residues were replaced by alanine (flag-sdc4S3A) and that therefore has no GAG side chains.

The next day, cells were incubated with 100 ng IL-1beta or TNF alpha (both R&D) for 1 h at 37 °C in DMEM medium without FCS. IL-1 was detected using an IL-1beta Antibody (#12242, Cell signaling) and TNF using a TNF alpha antibody (#3707, Cell signaling). True Blot secondary antibodies (Rockland) were used to ensure, that IgG fragments from the antibodies attached to the beads were not detected.

Isolation of caveolae

Isolation of caveolae was done according to the protocol of Ostrom and Insel [20] by sucrose gradient centrifugation. All the buffers used were identical to the protocol and proteinase inhibitors as well as phosphatase inhibitor were present in the lysis buffer, sucrose/MBS and Triton-X 100 buffer. After cell homogenization of a complete, confluent cell culture flask, the lysate was loaded on the described sucrose gradient and centrifugation was performed at 260,000 g for 18 h at 4 °C. Then, the gradient was separated into 250 µl fractions and ethanol precipitation was performed.

As lipid rafts and caveolae were more buoyant than other cellular parts, fraction 2 between the 35 % to 5% sucrose borderline was analysed using western blot analysis.

Western blotting

Total cell extracts were obtained using NP-40 buffer (150 mM sodium chloride, 1 % NP-40, 50 mM Tris HCl pH 8) containing protease inhibitor cocktail (Roche) and phosphatase inhibitor (Roche). The extracts were resolved by SDS-PAGE and transferred to a polyvinylidene difluoride membrane (GE Healthcare). The proteins were detected with appropriate antibodies using the ECL detection system (GE Healthcare) or Super Signal West Femto (Life Technologies). Antibodies against the following proteins were used: Scd4 (Pineda), Caveolin-1 (Abcam), p-Caveolin-1 (Tyr14), Erk1/2, p-Erk1/2, il-1beta, and TNFalpha (all from Cell signaling).

FACS Analysis

Confluent FLS cells were washed once with PBS and harvested by incubating the monolayer in 10 ml PBS containing 0.02% EDTA and detaching cells by firmly rocking. Unspecific staining was reduced by incubating the re-suspended cells in HBSS containing 1% BSA, 2% bovine FCS and 0.1% NaN_3 in the presence of 0.2 µl/well Fc blocking antibody (BD Biosciences) for 10 min on ice. For TNFR1 staining, 40 µl cell suspension in HBSS plus supplements were incubated with anti-TNFRI antibody (Abcam) or the equal concentration of isotype control rabbit IgG (R&D systems.) A secondary anti-rabbit A488 antibody (Life Technologies) was used. For IL1R1 staining the anti-IL1R1 PE antibody (BD Biosciences) or the respective isotype control (BD Biosciences) was used. For both stainings, dead cells were excluded by incubating with DAPI (Life Technologies) before recording on a FACS Canto II cytometer.

ELISA

Wt and Sdc4-/- synovial fibroblasts were cultured in DMEM (Sigma) supplemented with 10 % FCS (PAA). Confluent cells were stimulated with 10 ng murine IL-1 beta or 100 ng murine TNF alpha (R&D systems) for 8 h. Cell culture supernatants were assessed for total MMP-3 by ELISA (R&D systems) according to the manufacturers protocol.

siRNAs and transfection

Caveolin-1 siRNA was synthesized by Dharmacon (Lafayette, CO, USA) under the reference ON-TARGETplus Mouse Cav1 siRNA (J-058415-05-0050). Transfection of siRNAs was performed using N-TER nanoparticle siRNA transfection system (Sigma) according to the manufacturer's instructions. Wt synovial fibroblasts were transfected again after 48 h and cells were used after 72 h for western blot analysis.

Inhibition of caveolin vesicle formation via Nystatin

Formation of caveolin vesicles was inhibited using Nystatin (Sigma). Nystatin powder was dissolved in DMSO in a concentration of 10 mg/ml and used in a final concentration of 20 µg/ml dissolved in FCS-supplemented DMEM. Cells were pre-treated with Nystatin for 45 minutes prior to stimulation and overnight for flow cytometric analysis.

Semi-quantitative PCR from human and murine synovial fibroblasts

Total RNAs from SF was isolated using TRIzol reagent (Life technologies) according to the manufacturer's protocol. cDNAs were synthesized by reverse-transcriptase using the cDNA synthesis kit (Life technologies) with oligo dT primers. Primer sequences were as followed: Caveolin-1 forward 5'- AAC ATC TAC AAG CCC AAC AAC AAG G-3' and reverse 5'- GGT TCT GCA ATC ACA TCT TCA AAG TC-3'; GAPDH forward 5' AGC AAG GAC ACT GAG CAA GAG AGG 3' and reverse 5' GGG TCT GGG ATG GAA ATT GTG AGG 3'; il-1r forward 5' CCC GAG GTC CAG TGG TAT AAG AAC 3' and reverse 5´ ACT CCG AAG AAG CTC ACG TTG TC 3'; tnfrI forward 5' ACC TGT CAG TGA GGT AGT CCC AAC 3' and reverse 5' ACA GAA TCG CAA GGT CTG CAT TG 3', human scd4 forward 5´-cgg gca gga atc tga tga ctt tga-3´ and reverse: 5´-gct tca cgc gta gaa ctc att ggt-3´;

Proximity ligation assay

Gene synthesis of the complete murine syndecan-4 cDNA was performed by GeneArt (Invitrogen). Full length syndecan-4 cDNA was mutated such that the HA epitope was inserted between I^{32} and D^{33} of the extracellular domain. The cDNA was then cloned into the lentiviral vector pLNT-SFFV-MCS-eGFP and lentivirus produced in HEK293t cells using conventional procedures. NIH3T3 fibroblasts (HPA laboratories) were then transfected using the supernatant transfer method. NIH3T3 expressing Sdc4-HA-tagged (GFP^+) and untransfected cells were grown on 8-well chamber slides. Cells were treated for 5 min with 50 µl serum-free Optimem containing either 1:10 Rabbit anti-Sdc4 Ab (#1283, Lot 1405, 575 ng/µl), IL-1β (10 ng/ml) or both. Following treatments, medium was taken off, cells washed in PBS at RT, fixed in 4% PFA for 15' at RT. After a 5' wash in PBS, PFA was quenched by incubating cells with 0.1M NH_4Cl for 10min at RT. Proximity ligation assay was performed as per manufacturer's instructions (Duolink, Sigma Aldrich) using mouse IgG1 anti-HA Ab (Covance) and plus and minus anti-mouse probes. Images were taken using confocal

microscopy (Carl Zeiss LSM 700) with 63x oil objective and analysed using ImageJ software (NIH). Results were expressed as number of PLA dots per μm^2 of GFP^+ cells.

Cross linking

In order to stabilize the formed scd4 multimers, crosslinking was applied to cell surface proteins subsequent to multimerization experiments. Therefore, cells were washed four times with ice-cold PBS directly after IL-1 stimulation and then incubated with 1 - 5 mM of the crosslinking reagent BS3 (Thermo Fischer, Dreieich, Germany) at room temperature for 30 min. Finally, 15 mM Tris-HCl (pH 7.5) was added for 15 min to quench the reaction and after washing with PBS, the cells were directly lysed or frozen at -80 C.

Statistical analysis

All data are means ± SEM. Biological replicates are stated as n. Mean values of technical replicates are stated as n= 1. Statistical analysis was performed using GraphPad Prism Software, 6 (Graph Pad Software Inc., San Diego, CA, USA). Differences between groups were examined for statistical significance using an ANOVA with post-hoc t-test and Bonferroni correction for multiple testing, or Welch's t-test; *p<0.05.

Acknowledgments:

We would like to thank A. Schröder, C. Schneider and M. Könnecke for technical support.

Funding

We would like to thank the DFG for funding (Emmy Noether BE4328/5-1 and FOR2722).

Patient and Public involvement

As this publication describes findings from basic research, we did not involve patients or the public in our study.

Competing interests

No conflict of interest

Contributorship

LG performed the main experiments, MB performed the IL-1 time dependent IL1R1 reduction in FACS, AKP performed the histological mouse model evaluation, UK established the IL1R1 FACS protocol, JS performed the phospho- caveolin western blot, DB performed the hTNFtg/ il1R1 breeding, KM performed the sdc4 stainings in murine und human RA sections, FE helped writing the manuscript and interpreting the data, JW and GDR did the dimerization experiments, TP and JB drafted the manuscript, evaluated the data and steered the project.

Ethical approval information

The ethics committees of the University Hospital Muenster approved all studies. Samples of synovial tissues from patients with RA or OA were obtained from joint replacement surgery (Ethics committee Muenster, approval number 2009-049-f-s).All animal experiments were authorized by the Animal Use Committee in Muenster under the file reference 84-02.04.2014.A465.

Data sharing statement

All relevant data are included in the article and will be made available upon request

References

1. Muller-Ladner U, Gay RE, Gay S. Molecular biology of cartilage and bone destruction. Curr Opin Rheumatol 10(3): 212, 1998

2. Pap T, Meinecke I, Muller-Ladner U, Gay S. Are fibroblasts involved in joint destruction? Ann Rheum Dis 64 Suppl 4: iv52, 2005

3. Pap T, Muller-Ladner U, Gay RE, Gay S. Fibroblast biology. Role of synovial fibroblasts in the pathogenesis of rheumatoid arthritis. Arthritis research 2(5): 361, 2000

4. Burger D, Dayer JM, Palmer G, Gabay C. Is IL-1 a good therapeutic target in the treatment of arthritis? Best Pract Res Clin Rheumatol 20(5): 879, 2006

5. Zwerina J, Redlich K, Polzer K, Joosten L, Kronke G, Distler J, Hess A, Pundt N, Pap T, Hoffmann O, Gasser J, Scheinecker C, Smolen JS, van den Berg W, Schett G. TNF-induced structural joint damage is mediated by IL-1. Proceedings of the National Academy of Sciences of the United States of America 104(28): 11742, 2007

6. Echtermeyer F, Bertrand J, Dreier R, Meinecke I, Neugebauer K, Fuerst M, Lee YJ, Song YW, Herzog C, Theilmeier G, Pap T. Syndecan-4 regulates ADAMTS-5 activation and cartilage breakdown in osteoarthritis. Nature medicine 15(9): 1072, 2009

7. Korb-Pap A, Stratis A, Muhlenberg K, Niederreiter B, Hayer S, Echtermeyer F, Stange R, Zwerina J, Pap T, Pavenstadt H, Schett G, Smolen JS, Redlich K. Early structural changes in cartilage and bone are required for the attachment and invasion of inflamed synovial tissue during destructive inflammatory arthritis. Ann Rheum Dis 71(6): 1004, 2012

8. Oakley FD, Smith RL, Engelhardt JF. Lipid rafts and caveolin-1 coordinate interleukin-1beta (IL-1beta)-dependent activation of NFkappaB by controlling endocytosis of Nox2 and IL-1beta receptor 1 from the plasma membrane. The Journal of biological chemistry 284(48): 33255, 2009

9. Williamson RC, Cowell CA, Reville T, Roper JA, Rendall TC, Bass MD. Coronin-1C Protein and Caveolin Protein Provide Constitutive and Inducible Mechanisms of Rac1 Protein Trafficking. The Journal of biological chemistry 290(25): 15437, 2015

10. Bass MD, Williamson RC, Nunan RD, Humphries JD, Byron A, Morgan MR, Martin P, Humphries MJ. A syndecan-4 hair trigger initiates wound healing through caveolin- and RhoG-regulated integrin endocytosis. Developmental cell 21(4): 681, 2011

11. Couchman JR, Woods A. Syndecan-4 and integrins: combinatorial signaling in cell adhesion. Journal of cell science 112 (Pt 20): 3415, 1999

12. Bass MD, Humphries MJ. Cytoplasmic interactions of syndecan-4 orchestrate adhesion receptor and growth factor receptor signalling. Biochem J 368(Pt 1): 1, 2002

13. Bertrand J, Bollmann M. Soluble syndecans: biomarkers for diseases and therapeutic options. Br J Pharmacol 176(1): 67, 2019

14. Ramsden L, Rider CC. Selective and differential binding of interleukin (IL)-1 alpha, IL-1 beta, IL-2 and IL-6 to glycosaminoglycans. Eur J Immunol 22(11): 3027, 1992

15. Choi Y, Yun JH, Yoo J, Lee I, Kim H, Son HN, Kim IS, Yoon HS, Zimmermann P, Couchman JR, Cho HS, Oh ES, Lee W. New structural insight of C-terminal region of Syntenin-1, enhancing the molecular dimerization and inhibitory function related on Syndecan-4 signaling. Sci Rep 6: 36818, 2016

16. Shin J, Lee W, Lee D, Koo BK, Han I, Lim Y, Woods A, Couchman JR, Oh ES. Solution structure of the dimeric cytoplasmic domain of syndecan-4. Biochemistry 40(29): 8471, 2001

17. Lajoie P, Nabi IR. Lipid rafts, caveolae, and their endocytosis. Int Rev Cell Mol Biol 282: 135, 2010

18. Bass MD, Morgan MR, Humphries MJ. Integrins and syndecan-4 make distinct, but critical, contributions to adhesion contact formation. Soft matter 3(3): 372, 2007

19. Keffer J, Probert L, Cazlaris H, Georgopoulos S, Kaslaris E, Kioussis D, Kollias G. Transgenic mice expressing human tumour necrosis factor: a predictive genetic model of arthritis. EMBO J 10(13): 4025, 1991

20. Ostrom RS, Insel PA. Methods for the study of signaling molecules in membrane lipid rafts and caveolae. Methods Mol Biol 332: 181, 2006

Figure legends.

Figure 1: Scd4 reduces IL-1ß signalling by direct binding to the HS side chains and induction of sdc4 dimerization. a, Representative images of enhanced syndecan-4 staining in tissue sections from rheumatoid patients (RA) compared to osteoarthritic patients (OA) (red, 200x magnification) (n= 10). Quantitative real-time PCR of syndecan-4 mRNA levels in RASF and OASF revealed upregulation of syndecan-4 in RA patients (n=10, $p<0.05$). b, Representative immunohistochemical staining of synovial tissue sections of hTNFtg and wild type mice with monoclonal syndecan-4 antibody showed a high syndecan-4 expression in the pannus tissue (red, 200x magnification) (n= 8). Quantitative real-time PCR showed a 21.6-fold upregulation in synovial fibroblasts of hTNFtg mice as compared to synovial fibroblasts of wild type mice normalized to HPRT (n= 4). c, TNFalpha stimulation of wt and sdc4-/- synovial fibroblasts revealed no difference in Erk1/2 activation (n≥ 3). d, Sdc4-/- synovial fibroblasts showed a reduced Erk1/2 activation in response to IL-1 stimulation compared to wt (n≥ 3). e, Wt and Sdc4-/- synovial fibroblasts were stimulated with TNFalpha (n≥ 3), (f) or IL-1β and supernatants were used for MMP-3 ELISA (n≥3 , $*p<0.05$). g, Representative western blot of HEK cells were transfected with FLAG tagged full length sdc4 (flag-sdc4wt) or with a FLAG-tagged mutant of sdc4 holding no GAG side chains (flag-sdc4S3A). IL-1, however, could be detected in the eluate of the GAG side chain-holding construct (flag-sdc4wt), but not from the side chain-lacking construct (flag-sdc4S3A). h, Representative western blot of IL-1-induced sdc4 dimerization is independent of IL1R1. i, Representative western blot of Sdc4 dimerization induced by IL-1β. Figure a and b were analysed for statistical significance using a Welch's t-test. Figure c, d, e and f were analysed using an ANOVA with post-hoc t-test.

Figure 2: Sdc4 regulates IL1R1 trafficking upon IL-1 stimulation. a, FACS analysis revealed that IL-1R1 surface presentation was significantly reduced in Sdc4 deficient synovial fibroblasts (n=3, $*p<0.05$). b, Quantitative real-time PCR showed no difference in IL-1R1 mRNA expression levels comparing wt and Sdc4-/- synovial fibroblasts normalized to GAPDH (n≥5, $*p<0.05$). c, TNFR1 surface presentation was comparable between wt and Sdc4-/- synovial fibroblasts as shown by FACS analysis (n=3 , $*p<0.05$). d, TNFR1 mRNA expression was equal comparing wt, Sdc4-/- and IL1R1-/- synovial fibroblasts by quantitative real-time PCR (n≥5, $*p<0.05$). e, FACS analysis of IL-1R1 surface presentation was significantly reduced in wt synovial fibroblasts after 10 minutes of IL-1 stimulation, whereas no change was observed in Sdc4 deficient fibroblasts (n=4, $*p< 0.05$). f, The caveolin inhibitor Nystatin reduced activation of Erk1/2 in wt synovial fibroblasts in response to IL-1 stimulation. g, Knockdown of caveolin-1 using RNAi abolished activation of Erk1/2 in wt synovial fibroblasts. h, Pre-incubation with Nystatin reduced IL1R1 surface presentation in wt

synovial fibroblasts to the levels on Sdc4-/- cells (n=3). i, Quantitative real-time PCR showed no difference in caveolin-1 mRNA levels comparing wt and Sdc4-/- FLS (n≥5, *p<0.05). j, Sucrose gradient centrifugation was used to isolate caveolin vesicles after stimulation with IL-1. The representative western blot analysis showed a reduced caveolin phosphorylation in wt compared to Sdc4-/- synovial fibroblasts (n= 2). Data were analysed for statistical significance using an ANOVA with post-hoc t-test.

Figure 3: Sdc4 blocking antibody reduces IL1R1 surface presentation leading to reduced RA symptoms in the hTNFtg RA mouse model. a, Inhibition of sdc4 function by a polyclonal antibody directed against the membrane proximal part of the extracellular domain of sdc4 (anti-Sdc4-Ab) resulted in a diminished Erk1/2 activation in wt synovial fibroblasts. b, FACS staining revealed that a pre-incubation of wt synovial fibroblasts with anti-Sdc4-Ab led to a significant reduction of IL1R presentation compared to IgG treated cells (n=3, *p<0.05). c, Syndecan-4 dimerization is inhibited by IL1β stimulation and the blocking α-syndecan-4 antibody. Proximity ligation assays in NIH/3T3 cells transfected with HA tagged syndecan-4 reveal fewer dots per area (red) in the presence of both IL1β and syndecan-4 antibody (n=4, *p<0.05). d, hTNFtg mice were treated with our blocking anti-Sdc4- Antibodies (anti-Sdc4-Ab) or non-specific IgG (IgG control) from week 8 to week 12 of age, while hTNFtg x IL1R1-/- mice served as control. Representative Toluidine blue and MMP-3 stainings of hind paw sections of 12 weeks old hTNFtg mice are shown. Anti-Sdc4-Ab treatment of hTNFtg mice caused a strong decrease in MMP-3 levels (red) and inflammation as well as cartilage damage Mean areas of synovial pannus tissue, destaining of the cartilage (in percent of total cartilage), cartilage erosion (in percent of cartilage) and MMP-3 positive joint area in the tarsal joints was measured. Treatment of hTNFtg mice with anti-Sdc4-Ab showed decreased pannus formation and reduced MMP-3 levels (red) resulting in the preservation of cartilage in comparison to IgG treated hTNFtg mice (n≥4, *p<0.05 at week 12). Figure b, c, and d were analysed for statistical significance using an ANOVA with post-hoc t-test.

Suppl. Figure 1: Specificity of blocking sdc-4 antibodies. a.) Western blot with sdc4-/- and wildtype (wt) fibroblasts using the sdc-4 blocking antibody 1 to detect sdc4. No signal was observed in the sdc4-/- fibroblasts. b.) Immunocytochemistry of wt and sdc4-/- fibroblasts using the sdc-4blocking antibody 1. Again, no staining was observed in the sdc4-/- fibroblasts. c.) Western blot with sdc4-/- and wildtype (wt) fibroblasts using the sdc-4 blocking antibody 2 to detect sdc4. No signal was observed in the sdc4-/- fibroblasts. d.) Inhibition of sdc4 function by the sdc4 blocking antibody 2 resulted in a diminished IL-1 induced Erk1/2 activation in wt synovial fibroblasts.

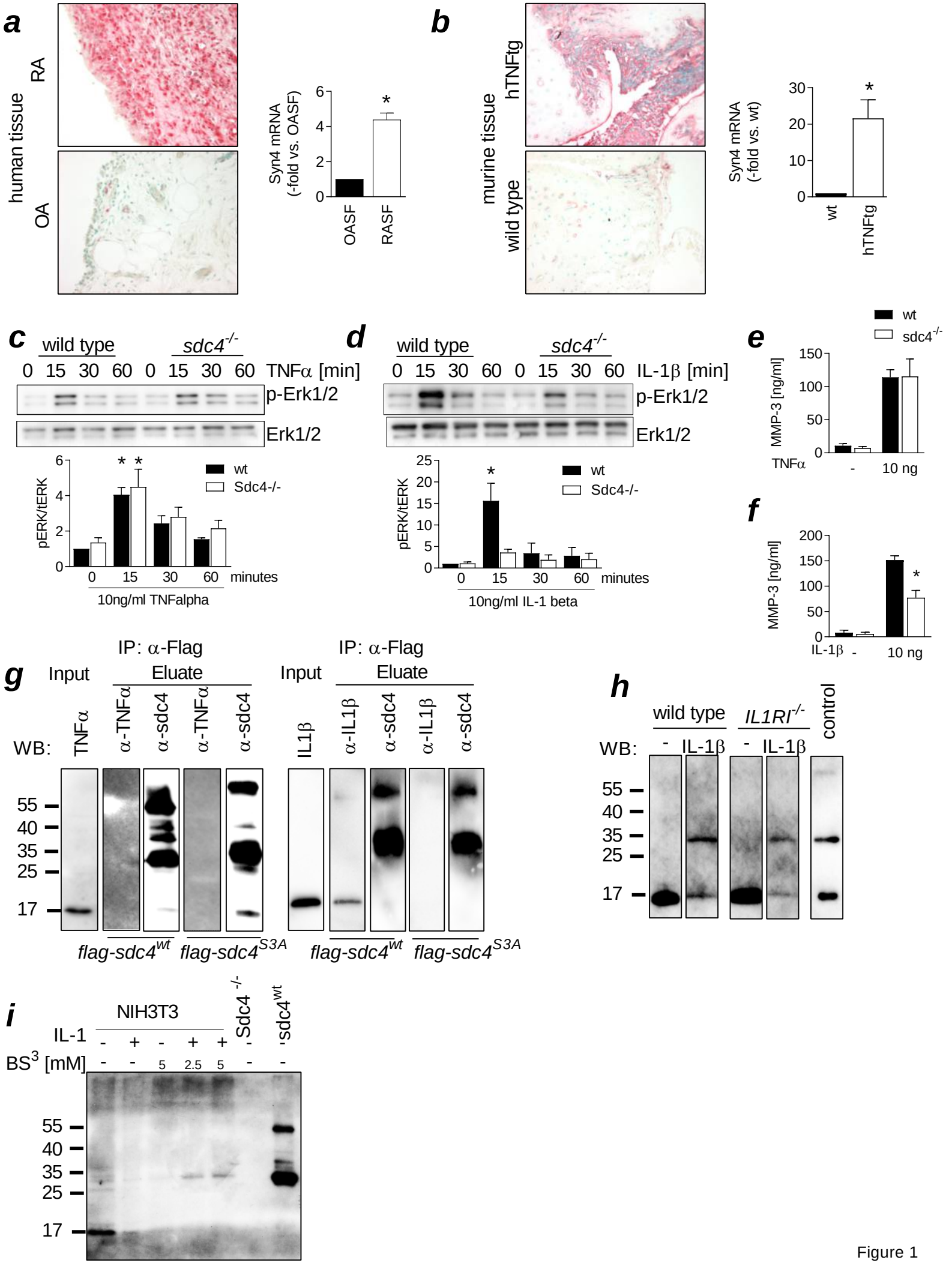
a
human tissue
RA
OA
Syn4 mRNA (-fold vs. OASF)
OASF
RASF
b
murine tissue
hTNFtg
wild type
Syn4 mRNA (-fold vs. wt)
wt
hTNFtg
c
wild type
sdc4-/-
0 15 30 60 0 15 30 60 TNFα [min]
p-Erk1/2
Erk1/2
pERK/tERK
wt
Sdc4-/-
minutes
10ng/ml TNFalpha
d
wild type
sdc4-/-
0 15 30 60 0 15 30 60 IL-1β [min]
p-Erk1/2
Erk1/2
pERK/tERK
wt
Sdc4-/-
minutes
10ng/ml IL-1 beta
e
wt
sdc4-/-
MMP-3 [ng/ml]
TNFα
- 10 ng
f
MMP-3 [ng/ml]
IL-1β - 10 ng
g
IP: α-Flag
Input
Eluate
WB:
TNFα
α-TNFα
α-sdc4
IL1β
α-IL1β
flag-sdc4wt
flag-sdc4S3A
h
wild type
IL1RI-/-
control
WB:
- IL-1β
i
NIH3T3
IL-1
BS3 [mM]
Sdc4-/-
sdc4wt

Figure 1

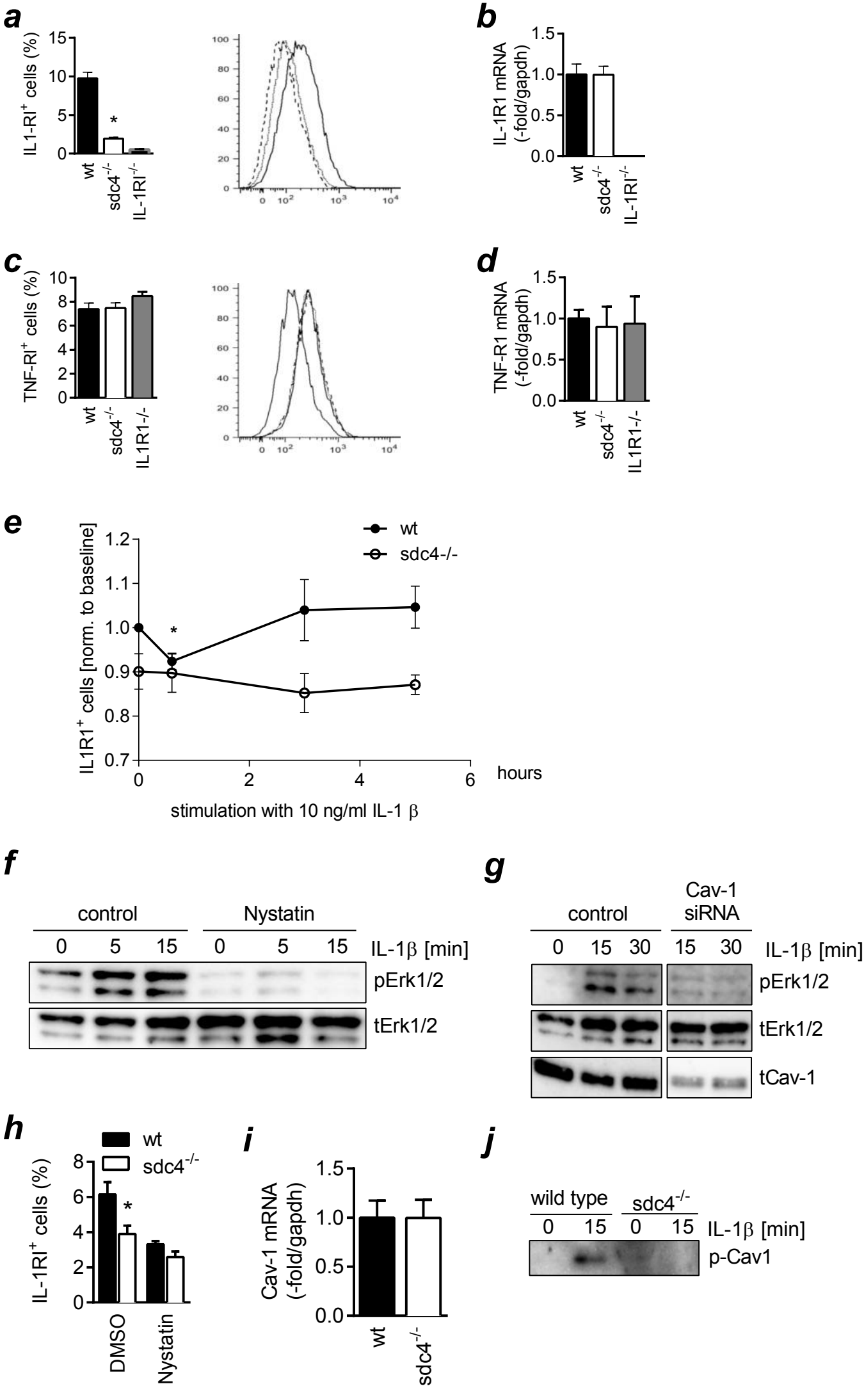
a
IL1-RI+ cells (%)
wt
sdc4-/-
IL-1RI-/-
b
IL-1R1 mRNA (-fold/gapdh)
c
TNF-RI+ cells (%)
IL1R1-/-
d
TNF-R1 mRNA (-fold/gapdh)
e
wt
sdc4-/-
IL1R1+ cells [norm. to baseline]
hours
stimulation with 10 ng/ml IL-1 β
f
control
Nystatin
IL-1β [min]
pErk1/2
tErk1/2
g
Cav-1 siRNA
tCav-1
h
DMSO
Nystatin
i
Cav-1 mRNA (-fold/gapdh)
j
wild type
p-Cav1

Figure 2

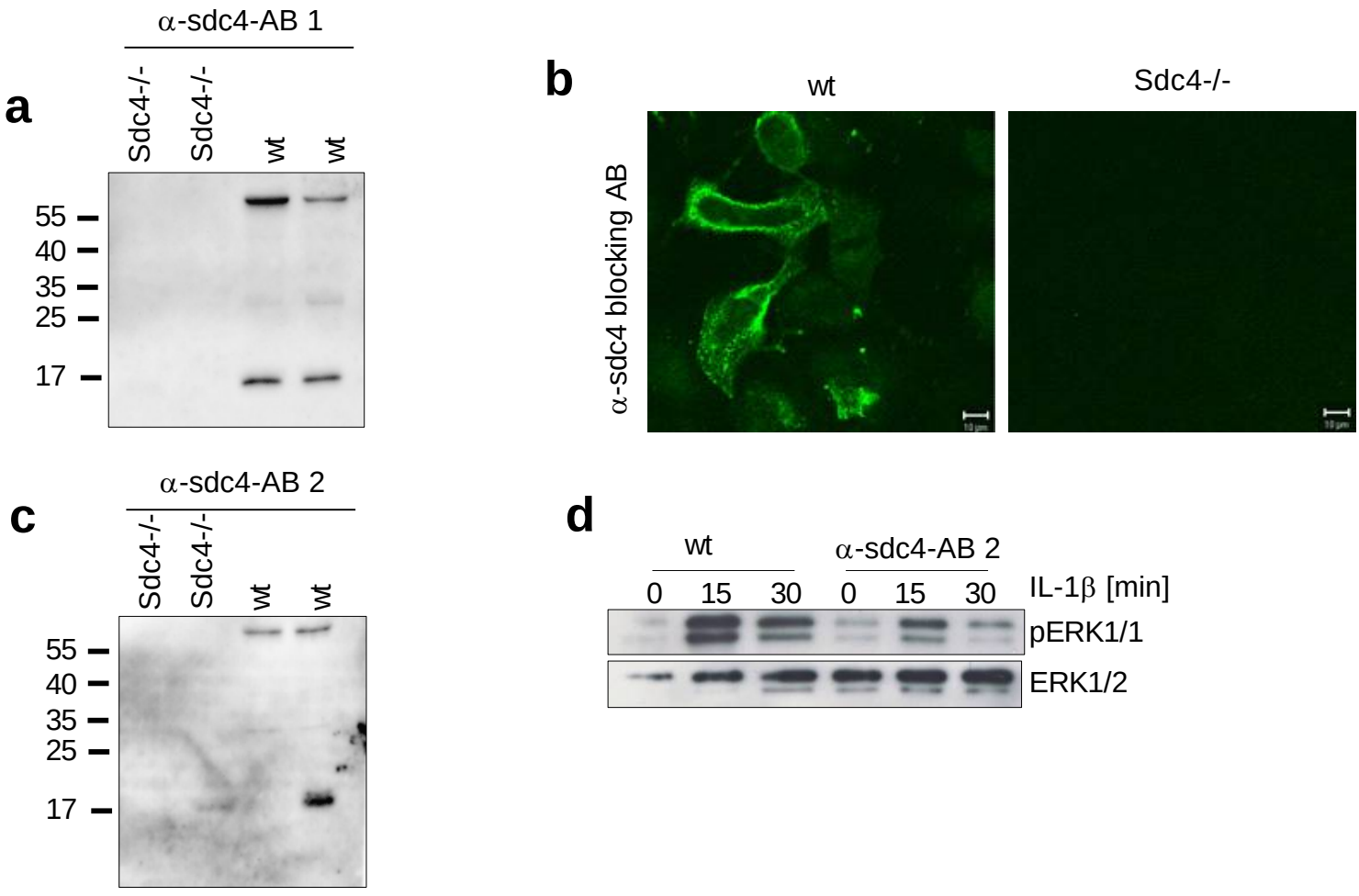

Suppl. figure 1

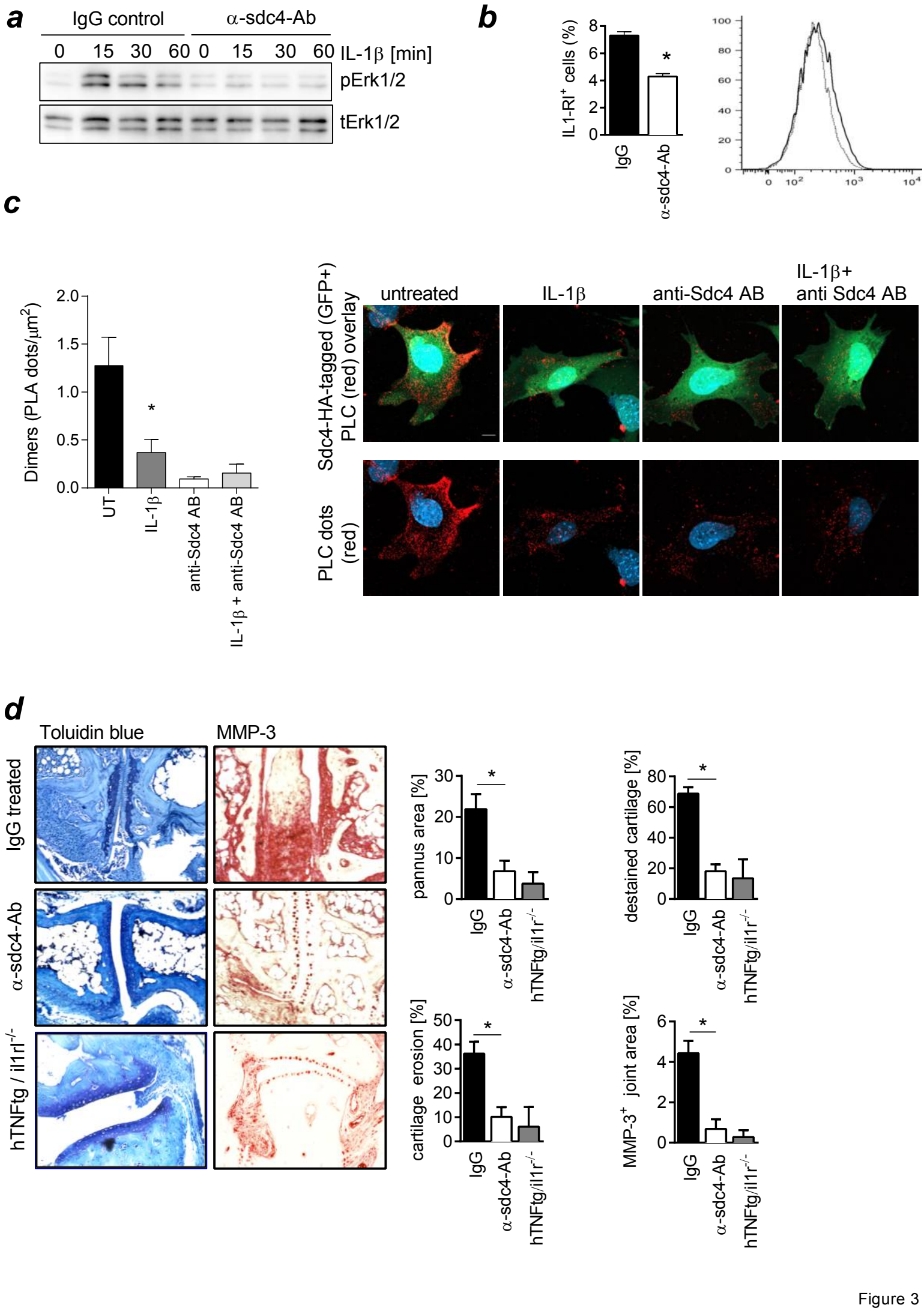
a
IgG control
α-sdc4-Ab
0 15 30 60 0 15 30 60 IL-1β [min]
pErk1/2
tErk1/2
b
IL1-RI+ cells (%)
IgG
α-sdc4-Ab
c
Dimers (PLA dots/μm2)
UT
IL-1β
anti-Sdc4 AB
IL-1β + anti-Sdc4 AB
untreated
IL-1β
anti-Sdc4 AB
IL-1β+ anti Sdc4 AB
Sdc4-HA-tagged (GFP+) PLC (red) overlay
PLC dots (red)
d
Toluidin blue
MMP-3
IgG treated
α-sdc4-Ab
hTNFtg / il1rl-/-
pannus area [%]
destained cartilage [%]
cartilage erosion [%]
MMP-3+ joint area [%]
IgG
α-sdc4-Ab
hTNFtg/il1r-/-

Figure 3